10.24425/acs.2026.1537

Archives of Control Sciences
Volume 36(LXXII), 2026
No. 2*, pages 251–276*

Poly-optimization of parameters of fractional-order power system stabilizers operating in the power system

Adrian NOCOŃ , Stefan PASZEK and Piotr PRUSKI

This paper presents a new fractional-order power system stabilizer, PSS3B_FRAC, developed as a modification of the standard PSS3B stabilizer. Optimization-based procedures are applied to determine stabilizer parameters in single-machine and multi-machine systems. The results demonstrate that introducing fractional-order differentiation improves damping of electromechanical swings while maintaining acceptable voltage regulation. The study is conducted in three stages: (1) single-objective optimization in single-machine systems, (2) single-objective optimization in a 7-machine CIGRE system, and (3) poly-optimization in the same system.

Key words: power system, power system stabilizers, fractional-order model, parameter optimization and poly-optimization, electromechanical swings

1. Introduction

In recent years, fractional-order differential calculus has been increasingly used to describe physical phenomena in various fields of knowledge. This calculus is based on the definitions of Gruenwald and Letnikov [2], Riemann–Liouville [1], and Caputo [11]. In electrical engineering, fractional calculus is used mainly in modeling supercapacitors [9,23] and inductors with ferromagnetic cores [17,39]. In control theory, fractional-order controllers [6] form a generalization of classical PID controllers, offering additional tuning flexibility through non-integer orders of integration and differentiation. They are distinguished by, among other things, the use of fractional-order integration and differentiation (with a specific real

A. Nocoń (e-mail: adrian.nocon@eviaverd.pl) is with Eviaverd Solutions, Składowa 10B, 42-690 Boruszowice, Poland.

S. Paszek (e-mail: stefan.paszek@polsl.pl) and P. Pruski (corresponding author, e-mail: piotr.pruski@polsl.pl) are with Faculty of Electrical Engineering, Silesian University of Technology, Akademicka 10, 44-100 Gliwice, Poland.

Received 15 November 2025. Revised 23 February 2026.

value) to achieve better control quality by increasing the number of available parameters of such a controller. Fractional-order controllers usually allow for achieving better control quality (in terms of selected quality factors) compared to traditional controllers [4, 6].

In the literature on modeling the elements of generating units of the power system (PS), there are few items related to fractional order models of synchronous generators [34] and regulators operating in the main circuit of excitation systems [41].

This paper discusses the use of fractional-order power system stabilizers (PSSs) to damp electromechanical swings [15, 16], i.e., slowly varying swings of synchronous generator rotors. These swings can also be observed in the instantaneous power waveforms of generators and transmission lines [25, 31]. In unfavorable cases, electromechanical swings can cause a loss of angular stability of generating units and, consequently, their emergency shutdown [36, 37].

One way to damp electromechanical swings, and thus also improve the angular stability of the system, is to use appropriately selected power system stabilizers [33, 35]. These stabilizers, which are part of the excitation systems, are designed to damp electromechanical swings by creating an additional damping component of the electromagnetic torque of the generators [15, 16]. However, applying PSSs may adversely affect voltage waveforms at individual nodes [25, 31].

In PS, traditional PSS3B system stabilizers are widely used [30, 32], which have two input signals, proportional to the instantaneous (active) power and to the deviation of the angular speed of the generator, and a simple structure [30, 32].

The use of a fractional-order power system stabilizer derived from the classical PSS3B structure has been proposed and denoted as PSS3B_FRAC. In the literature, numerous alternative fractional-order PSS concepts have also been developed. These include adaptive fractional sliding-mode-based stabilizers aimed at improving robustness against disturbances and parameter uncertainties [5], adaptive fractional-order PID-based PSS solutions enhancing transient stability of Single Machine Infinite Bus (SMIB) systems under varying operating conditions [13], coordinated tuning of PSS with wide-area measurement-based fractional-order PID controllers for damping low-frequency oscillations in large-scale PV-integrated smart grids [38], fractional-order AVR–PSS lead–lag compensator structures designed for improved damping performance [42], and robust fractional-order PSS formulations validated through eigenvalue and nonlinear time-domain analyzes [43].

This paper presents the optimization of PSS3B_FRAC power system stabilizer parameters. Example calculations were performed in three stages: 1) single-objective optimization in single-machine systems, 2) single-objective optimization in a seven-machine PS CIGRE, 3) poly-optimization (multi-objective optimization) in PS CIGRE.

2. Fractional-order stabilizer PSS3B_FRAC

Each signal control path of a traditional PSS3B stabilizer consists of a derivative element, a correction coefficient, and a gain. Limiting the stabilizer's output signal is used to eliminate the stabilizer's significant influence on the voltage control channel.

In the PSS3B_FRAC stabilizer, it was proposed to replace the traditional correction terms of the type $\dfrac{1}{1+sT}$ in both control path with correction terms of the type $\dfrac{1}{1+s^{\alpha}T}$, where α is a real number defining the derivative order. The derivative terms used to eliminate the constant component were left unchanged. The structural diagram of the PSS3B_FRAC stabilizer is shown in Figure 1.

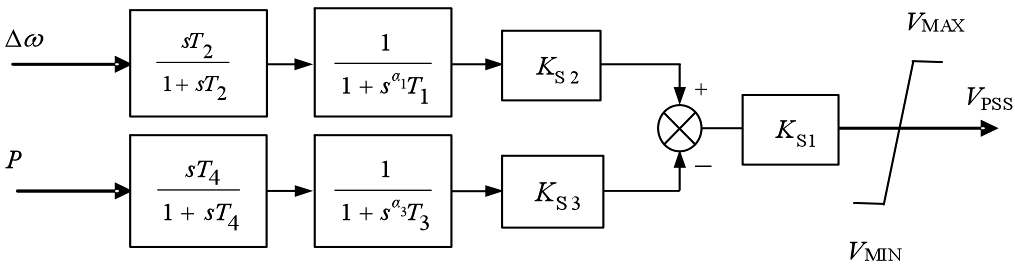

Figure 1: Structural diagram of power system stabilizer PSS3B_FRAC, ω, P, V_{PSS} – angular speed, instantaneous (active) power of the generator, stabilizer output signal

During optimization investigations of single-signal power system stabilizers and dual-input PSS2A [10, 31] stabilizers, the time constants of their correction elements were selected so that the component of the generator's electromagnetic torque, controlled by the stabilizer, had the character of a damping torque [8], i.e. was proportional to the deviation of the generator's angular speed [15, 20]. The simple structure of the traditional PSS3B [10, 30] and PSS3B_FRAC stabilizers does not allow for determining appropriate compensation conditions [15, 16]. Therefore, the selection of the parameters of the PSS3B_FRAC and PSS3B stabilizers can lead to minimization of the appropriate objective functions, determined by the waveforms of the instantaneous power, angular speed and voltage of the generators.

The introduction of additional parameters in the PSS3B_FRAC stabilizer model, related to the fractional-order derivative blocks in the input paths of the system, should improve the performance of this stabilizer compared to the PSS3B stabilizer.

In the further part of the paper, to simplify the research, in the PSS3B_FRAC stabilizer model, the fractional order element was used only in the instantaneous power control path.

3. Single-objective optimization of the stabilizers parameters

Power system stabilizers are designed to damp electromechanical swings, i.e., changes in the instantaneous power and angular speed waveforms of synchronous generators [25]. Therefore, deviations from the steady-state values should be minimized during transients. Furthermore, the introduction of stabilizers must not adversely affect the voltage regulation waveforms at the generator terminals. Consequently, determining the optimal parameters of the PSS3B_FRAC and PSS3B stabilizers can be reduced to minimizing the appropriate objective function.

In the case of analysis of a single-machine system of the generating unit – infinite bus type, with a typical disturbance: a transient symmetrical short circuit in the transmission line or a step change in the voltage regulator reference voltage, the objective function can be presented in the form [30, 31]:

$$f_{\mathrm{S}}\left(\boldsymbol{x}_{\mathrm{S}}\right)=\sum_{i=1}^{n}\left|w_{\mathrm{p}}\Delta P_{i}\left(\boldsymbol{x}_{\mathrm{S}}\right)\right|^{2}+\left|w_{\omega}\Delta\omega_{i}\left(\boldsymbol{x}_{\mathrm{S}}\right)\right|^{2}+\left|w_{\mathrm{V}}\Delta V_{i}\left(\boldsymbol{x}_{\mathrm{S}}\right)\right|^{2}, \tag{1}$$

where: $\boldsymbol{x}_{\mathrm{S}}$ – vector of the optimized parameters of one power system stabilizer, ΔP_i, $\Delta\omega_i$, ΔV_i – deviations of active power, angular speed and generator voltage in successive i-th time instants, n – number of samples of the analyzed waveforms, w_{p}, w_{ω}, w_{V} – weighting coefficients.

When analyzing a multi-machine PS, the following objective function can be introduced [30, 31]:

$$f(\boldsymbol{x})=\sum_{j=1}^{N_i}\sum_{i=1}^{n}\left|w_{\mathrm{p}j}\Delta P_{ij}(\boldsymbol{x})\right|^{2}+\left|w_{\omega j}\Delta\omega_{ij}(\boldsymbol{x})\right|^{2}+\left|w_{\mathrm{V}j}\Delta V_{ij}(\boldsymbol{x})\right|^{2}, \tag{2}$$

where: $\boldsymbol{x}$ – vector of optimized parameters of power system stabilizers introduced in particular generating units, N_i – number of generating units in the PS, ΔP_{ij}, $\Delta\omega_{ij}$, ΔV_{ij} – deviations of active power, angular speed and generator voltage in particular (j-th) generating unit (in p.u.) at the successive i-th time instants, $w_{\mathrm{p}j}$, $w_{\omega j}$, $w_{\mathrm{V}j}$ – weighting coefficients.

An important issue is the appropriate selection of weighting coefficients appearing in the minimized objective function, as their values significantly impact the obtained optimization results.

4. Poly-optimization of the stabilizers parameters

Poly-optimization (multi-objective optimization, vector optimization, multi-criteria optimization, Pareto optimization) is applied in engineering to solve problems for which an explicit quality factor does not exist. For example, it has been used for optimal tuning of non-linear stabilizers and power oscillation dampers using advanced metaheuristic algorithms [7], for coordinated design of PSS and supplementary damping controllers based on immune-inspired optimization techniques [12], and for simultaneous multi-scenario tuning of PSS parameters using Pareto-based approaches [24]. Poly-optimization is a kind of generalization of classical single-objective optimization [29].

Optimization (e.g. described in Section 3 of this paper) consists in improving one quality factor (minimizing a one-dimensional objective function), and the optimal solution is a set of optimal values of selected parameters [26, 29].

Objective functions, e.g., defined by expressions ((1) or (2)), subject to minimization, contain various components related to the optimized criteria. One of the fundamental problems in determining such objective functions is the appropriate selection of weighting coefficients corresponding to the individual function components [27]. Section 5 proposes methods for selecting these weighting coefficients (including equation (7)). However, this is only one of many possibilities for determining these coefficients, and many others could be proposed [25]. The analysis is further complicated by the presence of contradictory criteria (in such adopted objective functions): the criterion of minimizing changes in instantaneous power (including deviations in the angular speed of the generators) and the usually contradictory criterion of minimizing changes in the terminal voltage of individual generators [30, 31]. Moreover, the adopted values of the weighting coefficients in the additive objective function significantly influence the final optimization results.

A solution to this problem can be the use of multi-criteria optimization [26, 29]. It allows for the simultaneous consideration of different and contradictory criteria [30, 31]. Multi-objective optimization uses a vector criterion (instead of a single objective function). By conducting poly-optimization, a set of Pareto optimal solutions, i.e., a “compromise set” $\boldsymbol{\Lambda}$, is determined, which is the result of a simultaneous search for the extrema of many factors, called aspects, in the multidimensional objective space $\boldsymbol{F}$ [26, 29].

The exemplary compromise set for two-dimensional objective space is shown in Figure 2.

Assuming that the objective function in which nq components (single criteria) are taken into account, each of which is a function of n variables (in the considered case, parameters of the PSSs operating in the PS) in the general case, takes the

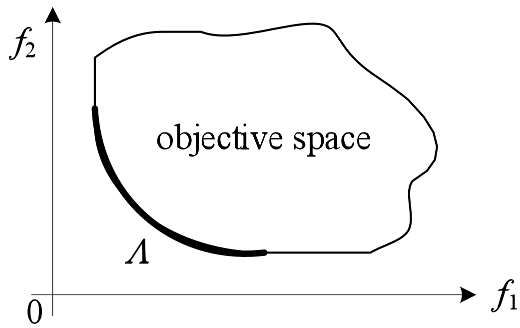

Figure 2: Exemplary compromise set for two-dimensional objective space

form:

$$\boldsymbol{f}=\begin{bmatrix} f_1(\boldsymbol{x}) \\ f_2(\boldsymbol{x}) \\ \vdots \\ f_i(\boldsymbol{x}) \\ \vdots \\ f_{nq}(\boldsymbol{x}) \end{bmatrix}=\begin{bmatrix} f_1(x_1,\cdots,x_j,\cdots,x_n) \\ f_2(x_1,\cdots,x_j,\cdots,x_n) \\ \vdots \\ f_i(x_1,\cdots,x_j,\cdots,x_n) \\ \vdots \\ f_{nq}(x_1,\cdots,x_j,\cdots,x_n) \end{bmatrix}, \tag{3}$$

where: $\boldsymbol{f}$ – objective function, $\boldsymbol{x}$ – vector of control variables (set of the PSSs parameters), f_i – value of the i-th component function for the set of parameters $\boldsymbol{x} = \left\{x_1,\cdots,x_j,\cdots,x_n\right\} \in \boldsymbol{X}$, $\boldsymbol{X}$ – control space (domain of the objective function, determined by the permissible values of the PSSs parameters), nq – number of the optimized component functions, n – number of the optimized variables (PSSs parameters).

The solution to such a defined minimization problem is not one optimal set of independent variables, but a set of sets $\widetilde{\boldsymbol{x}} = \left\{\widetilde{x}_1,\cdots,\widetilde{x}_j,\cdots,\widetilde{x}_n\right\} \in \boldsymbol{X}$ in which each of the elements is optimal in multi-criteria optimization. The set of the objective function values corresponding to the optimal parameters $\widetilde{\boldsymbol{x}}$ is called the compromise set (Pareto-optimal front). The set of compromises $\boldsymbol{\Lambda}$ includes all such points of the objective space $\left\{\widetilde{f_1},\widetilde{f_2},\ldots,\widetilde{f_{nq}}\right\} \in \boldsymbol{F}$, where: $\boldsymbol{F}$ – objective space, i.e. the area of possible values of the vector objective function (adaptation) $\boldsymbol{f}$, and the symbol $\widetilde{\cdot}$ denotes the optimal value in multi-criteria optimization, for which there is no direction of simultaneous improvement. The direction of the simultaneous improvement is such a change of the optimized variables $\boldsymbol{x}$, which results in the simultaneous improvement of all the components of the objective function f_i. The above definition, when minimizing the objective function, can be written as follows:

$$\begin{bmatrix} \widetilde{f}_1\left(\widetilde{\boldsymbol{x}}\right) \\ \widetilde{f}_2\left(\widetilde{\boldsymbol{x}}\right) \\ \vdots \\ \widetilde{f}_i\left(\widetilde{\boldsymbol{x}}\right) \\ \vdots \\ \widetilde{f}_{nq}\left(\widetilde{\boldsymbol{x}}\right) \end{bmatrix} = \widetilde{\boldsymbol{f}} \in \boldsymbol{\Lambda} \Leftrightarrow \neg\, \exists_{\boldsymbol{x} \in \boldsymbol{X} \wedge \boldsymbol{x} \neq \widetilde{\boldsymbol{x}}} \begin{cases} \widetilde{f}_1\left(\widetilde{\boldsymbol{x}}\right) \geqslant f_1\left(\boldsymbol{x}\right), \\ \widetilde{f}_2\left(\widetilde{\boldsymbol{x}}\right) \geqslant f_2\left(\boldsymbol{x}\right), \\ \qquad \vdots \\ \widetilde{f}_i\left(\widetilde{\boldsymbol{x}}\right) \geqslant f_i\left(\boldsymbol{x}\right), \\ \qquad \vdots \\ \widetilde{f}_{nq}\left(\widetilde{\boldsymbol{x}}\right) \geqslant f_{nq}\left(\boldsymbol{x}\right), \end{cases} \tag{4}$$

where: symbol $\neg\exists$ means, does not exist, $\boldsymbol{\Lambda}$ – set of compromises, $\widetilde{f}_i$ – value of the i-th component function belonging to the set of compromises.

Multi-objective numerical optimization is inherently challenging. Its implementation can benefit from algorithms that are natively suited to optimization under varying and conflicting criteria. In the authors' view, such methods include particle swarm optimization algorithms [3,45] and genetic algorithms [28,44]. In this study, a suitably modified genetic algorithm [27] is employed to minimize a vector objective function. Adapting the genetic algorithm to multi-objective optimization involves modifying the selection method. The genetic algorithm [14,22], structured as in Figure 3, adapted to optimize multiple criteria simultaneously, searches for the global minimum of the vector objective function within a given

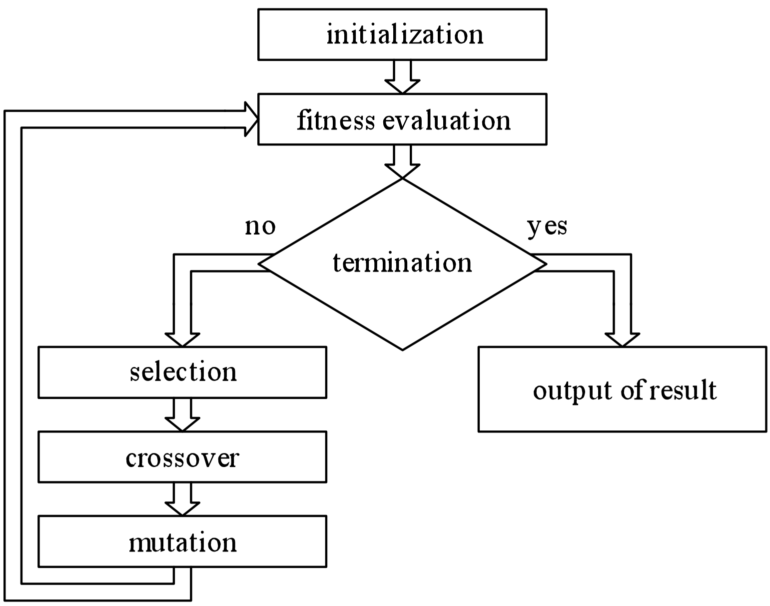

Figure 3: Structure of the genetic algorithm used in poly-optimization

range of determined parameters. The starting point is randomly selected from the search range, so there is no need to specify it precisely [21, 27].

Due to the complexity of phenomena occurring in the PS, the process of poly-optimizing the parameters of power system stabilizers should take into account many criteria related to the damping of electromechanical swings and the limitation of voltage changes in individual generating units during disturbances of the steady state [30, 31].

The vector objective function that is subject to minimization during poly-optimization of parameters of power system stabilizers operating in PS in a specific operating state and defined disturbance can be presented in the general form [27]:

$$\boldsymbol{f} = \begin{cases} \int |\Delta P_1(t)|^2 \, \mathrm{d}t \approx \sum\limits_{i=1}^{n} |\Delta P_{i1}|^2 \\ \vdots \\ \int \left|\Delta P_{N_i}(t)\right|^2 \, \mathrm{d}t \approx \sum\limits_{i=1}^{n} \left|\Delta P_{iN_i}\right|^2 \\ \int |\Delta V_1(t)|^2 \, \mathrm{d}t \approx \sum\limits_{i=1}^{n} |\Delta V_{i1}|^2 \\ \vdots \\ \int \left|\Delta V_{N_i}(t)\right|^2 \, \mathrm{d}t \approx \sum\limits_{i=1}^{n} \left|\Delta V_{iN_i}\right|^2 \\ \int |\Delta \omega_1(t)|^2 \, \mathrm{d}t \approx \sum\limits_{i=1}^{n} |\Delta \omega_{i1}|^2 \\ \vdots \\ \int \left|\Delta \omega_{N_i}(t)\right|^2 \, \mathrm{d}t \approx \sum\limits_{i=1}^{n} \left|\Delta \omega_{iN_i}\right|^2 \end{cases}, \tag{5}$$

where: N_i – number of generating units in the PS, ΔP_{ij}, $\Delta\omega_{ij}$, ΔV_{ij} – deviations of active (instantaneous) power, angular speed and generator voltage of the j-th generating unit (in p.u.) at the successive i-th time instants, n – number of samples of the analyzed waveforms, $j = 1 \ldots N_i$, N_i – number of generating units in the PS.

The final stage of poly-optimization involves selecting an optimal solution, typically achieved by comparing the obtained results within the N_i-dimensional objective space. When the dimensionality of this space is high, identifying the final solution becomes more difficult, and the optimization algorithms require increased computational effort. Therefore, the objective function (5) can be simplified by jointly determining the objective function values for a given physical quantity, expressed as follows:

$$\boldsymbol{f} = \begin{cases} \sum\limits_{j=1}^{N_i} \int \left|w_{pj} \Delta P(t)\right|^2 \mathrm{d}t \\ \sum\limits_{j=1}^{N_i} \int \left|\Delta V(t)\right|^2 \mathrm{d}t \\ \sum\limits_{j=1}^{N_i} \int \left|\Delta \omega(t)\right|^2 \mathrm{d}t \end{cases}, \tag{6}$$

where $w_{\mathrm{p}j}$ are weighting coefficients enabling normalization of the instantaneous power values when the rated powers of the individual j-th generators differ from each other (without these coefficients, the generator with the highest rated power would typically dominate the optimization outcome).

5. Results

5.1. Optimization calculations of stabilizers parameters in a single-machine system – stage 1

In order to perform the calculations, a model of the generating unit – infinite bus type (Figure 4) was developed in the Matlab-Simulink program [19].

This model was created by appropriately combining the models of a synchronous generator, excitation system, turbine, and power system stabilizer. The

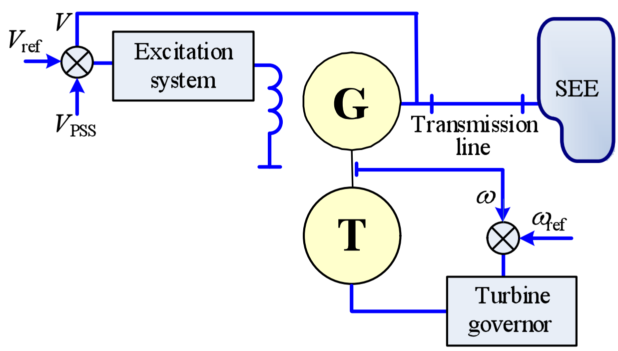

Figure 4: Schematic diagram of the generating unit, G – generator, T – turbine, ω_{ref} – reference angular speed, V – generator voltage, V_{ref} – reference voltage of the voltage regulator

selected models were: a synchronous generator – GENROU [30, 32], a static excitation system operating at the Polish Power System (PPS) [30], a steam turbine – IEEEG1 [30, 32], and a power system stabilizer – PSS3B or PSS3B_FRAC (Figure 5). *Fractional Variable Order Derivative Simulink Toolkit* [40] was used to calculate fractional-order derivatives in the Matlab-Simulink environment. A derivative implementation with a constant (time-invariant) derivative order value was implemented.

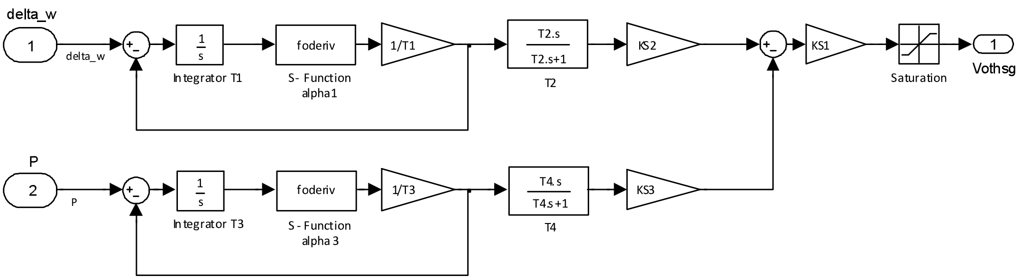

Figure 5: Schematic diagram of the PSS3B_FRAC stabilizer in the Matlab-Simulink environment

The following load conditions (active and reactive power) and typical values of the transmission line impedance Z_e (in p.u.) were taken into account in the optimization calculations:

- rating condition: $P_0 = 0.85$, $Q_0 = 0.5$;
- $Z_e = R_e + jX_e = 0.01 + j0.3$;
- $Z_e = R_e + jX_e = 0.01 + j0.6$.

A +5% step in the voltage regulator reference voltage V_{ref} was used as a representative small-signal disturbance to assess swing damping.

Based on experience and multi-variant preliminary studies, the following values of weighting coefficients in the objective function (1) were finally adopted: $w_p = 1$, $w_\omega = 100$, $w_V = 10$. The assumption of relatively high values of the weighting coefficients w_ω and w_V is caused, on the one hand, by small changes in the angular speed, and on the other hand, by the need to ensure satisfactory generator voltage regulation curves.

Optimization calculations for a single-machine system were performed separately for each generating unit of the 7-machine CIGRE power system shown in Figure 6. In the example calculations, it was assumed that the fractional-order element is located only in the instantaneous power control path of the PSS3B_FRAC stabilizer. This path has a greater impact on damping electromechanical swings than the generator angular speed deviation path.

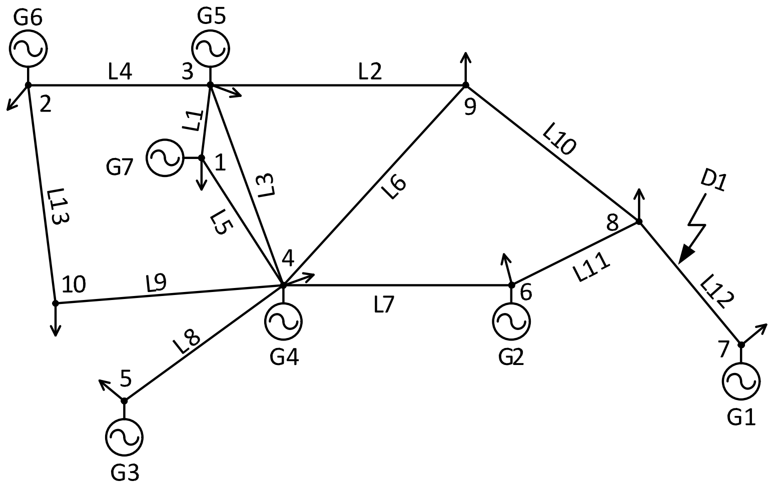

Figure 6: 7-machine CIGRE power system

To minimize the objective function (1), defined for individual generating units, the Newton gradient algorithm from the Optimization Toolbox of the Matlab program was used [18].

Tables 1 and 2 summarize the results of optimizing the parameters of the PSS3B and PSS3B_FRAC stabilizers in individual generating units, modeled as single-machine systems (units G5 and G6 have the same parameters, so the same calculation results were obtained). The obtained values of the objective function $f_S(\boldsymbol{x}_S)$ during optimization are also presented. Typical, constant values of the following parameters were assumed for both stabilizer types: $K_{S1} = 1$, $V_{MAX} = 0.2$ and $V_{MIN} = -0.066$. Relatively low gain values were also assumed in both control paths: $K_{S2} = 6.948$ and $K_{S3} = 0.03$. Adopting such gain values

Table 1: Calculation results of PSS3B stabilizer parameters in single-machine systems

Generating unit	T_1	T_2	T_3	T_4	$f_S(\boldsymbol{x}_S)$
G1	0.0100	0.1001	0.0174	0.7378	20.5734
G2	0.0100	0.1001	0.0210	0.5121	27.9374
G3	0.0100	0.1000	0.0243	0.2806	21.6969
G4	0.0100	0.1000	0.0100	0.2195	32.825
G5, G6	0.0100	0.1009	0.0173	0.7568	22.6606
G7	0.0100	0.2168	0.0424	4.9337	16.1176

results in relatively weak damping of swings, which allows for easier analysis of the effect of the remaining stabilizer parameters on the waveforms.

Table 2: Calculation results of PSS3B_FRAC stabilizer parameters in single-machine systems

Generating unit	T_1	T_2	T_3	T_4	α_3	$f_S(\boldsymbol{x}_S)$
G1	0.0100	0.1013	0.0137	0.9787	1.6874	20.3534
G2	0.0100	0.1000	0.0127	0.2893	1.8819	27.6437
G3	0.0100	0.1000	0.0113	0.1763	1.8925	21.5662
G4	0.0100	0.1000	0.0108	0.3430	1.0487	32.8273
G5, G6	0.0100	0.1000	0.0126	0.3414	1.8986	22.1587
G7	0.0100	0.2404	0.0153	2.0361	1.8445	14.8609

Figure 7 compares instantaneous power and terminal voltage waveforms for unit G5 with and without PSS, using parameters obtained from optimization, to illustrate the performance gain from PSS3B_FRAC over PSS3B.

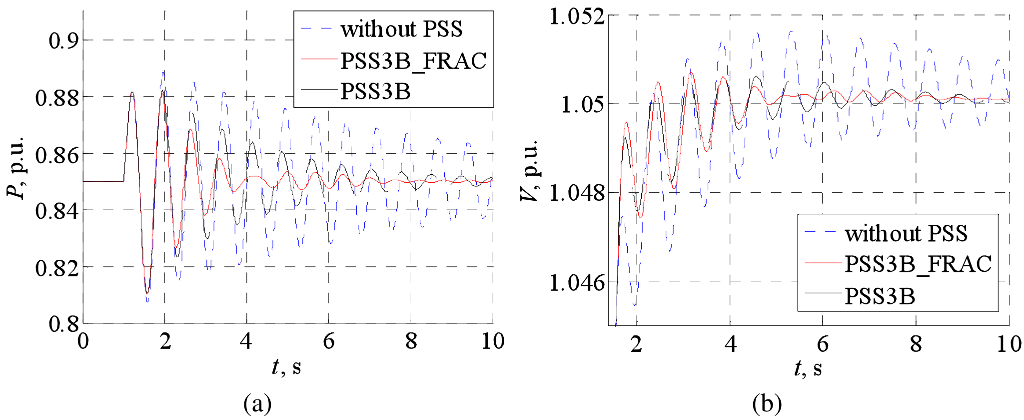

Figure 7: Waveforms of: instantaneous power (a) and generator voltage (b) in the G5 unit operating in a single-machine system

5.2. Single-criteria optimization calculations of stabilizer parameters in a multi-machine system – stage 2

Simulation and optimization calculations of the multi-machine system were performed for the 7-machine CIGRE system.

The weighting coefficients in the objective function (2) related to the active power can be made dependent on the rated power of individual generators [30]:

$$w_{\mathrm{p}j} = \frac{n_j S_{\mathrm{N}j}}{S_{\max}}, \tag{7}$$

where: n_j – number of generators operating in the j-th generating unit, $S_{\mathrm{N}j}$ – rated apparent power of a single synchronous generator operating in the j-th generating unit, $S_{\max}$ – rated apparent power of the generating unit that generates the highest apparent power in the considered load condition of the PS.

The relationships between the weighting coefficients associated with different quantities are also important. It is proposed to assume relatively large values of the weighting coefficients $w_{\omega j}$ and $w_{\mathrm{V}j}$ compared to the weighting coefficients $w_{\mathrm{p}j}$: $w_{\omega j} = 180 \cdot w_{\mathrm{p}j}$, $w_{\mathrm{V}j} = 35 \cdot w_{\mathrm{p}j}$, so that the components of the objective function (2), associated with individual quantities, have approximately equal values before optimization.

Larger weights were assigned to angular speed and voltage terms to compensate for their smaller absolute deviations and to balance the contributions of all components of Eq. (2) prior to optimization.

The disturbance was assumed to be a 50% change in the impedance of the L12 transmission line (marked D1 in Figure 6) with a duration of 0.25 s. Such a change in impedance may be related to a symmetric short circuit in the power grid located far away from the generating units. In the simulation studies, this type of disturbance was adopted because a temporary impedance variation (as opposed to an ideal short circuit with zero impedance) reduces the risk of large numerical errors in the computational model, while still constituting a sufficiently severe disturbance to effectively evaluate the performance of the PSS.

In the seven-machine CIGRE system, only the T_3 and α_3 parameters of the PSS3B_FRAC stabilizer were optimized to investigate the influence of fractional-order correction terms in the instantaneous power control circuit on the waveforms of the analyzed quantities. The initial values of these parameters and the remaining parameters resulted from the optimization performed in single-machine systems.

Newton's gradient algorithm was used to minimize the objective function (2).

Table 3 compares the parameters of the PSS3B_FRAC stabilizer and the value of the objective function (2) for the CIGRE system, after optimization in single-machine systems and after optimization in the CIGRE system.

Table 3 shows that by minimizing the objective function (2) in the second stage of calculations, it is possible to increase the damping of electromechanical swings and improve the nodal voltage waveforms in multi-machine power systems, which corresponds to a reduction in the objective function value of about 1.13%.

Table 3: Calculation results of PSS3B_FRAC stabilizer parameters in single-machine and 7-machine systems

	G1	G2	G3	G4	G5	G6	G7
Optimization in single-machine systems, $f(\boldsymbol{x}) = 1.37473$							
T_3	0.0137	0.0127	0.0113	0.0108	0.0126	0.0126	0.0153
α_3	1.6874	1.8819	1.8925	1.0487	1.8986	1.8986	1.8445
Optimization in the CIGRE multi-machine system, $f(\boldsymbol{x}) = 1.35936$							
T_3	0.0116	0.0144	0.0173	0.0631	0.0467	0.0209	0.0191
α_3	1.7923	1.8417	1.8361	1.1780	1.6143	1.9142	1.7976

5.3. Poly-optimization of stabilizer parameters in a multi-machine system – stage 3

Poly-optimization calculations were carried out for the same 7-machine CIGRE system and the same type of disturbance as in Section 5.2.

Considering that, in classical optimization, the objective function (2) consists of three additive components, the first case examines poly-optimization of a vector objective function comprising three component criteria:

$$\boldsymbol{f} = \begin{cases} f_1 \\ f_2 \\ f_3 \end{cases} = \begin{cases} f_{\mathrm{P}} \\ f_{\mathrm{V}} \\ f_{\omega} \end{cases} = \begin{cases} \sum\limits_{j=1}^{N_i} \sum\limits_{i=1}^{n} \left| w_{\mathrm{p}j} \Delta P_{ij} \right|^2 \\ \sum\limits_{j=1}^{N_i} \sum\limits_{i=1}^{n} \left| \Delta V_{ij} \right|^2 \\ \sum\limits_{j=1}^{N_i} \sum\limits_{i=1}^{n} \left| \Delta \omega_{ij} \right|^2 \end{cases} \tag{8}$$

where ΔP_{ij}, $\Delta\omega_{ij}$, and ΔV_{ij} denote the deviations of active (instantaneous) power, angular speed, and generator voltage of the j-th generating unit at successive i-th time instants, n – number of samples of the analyzed waveforms.

As in the case of classical optimization, 14 parameters were subject to poly-optimization, namely the T_3 and α_3 coefficients for all generating units.

Poly-optimization was carried out using a suitably modified genetic algorithm [27]. A genetic algorithm with real-number encoding, two-individual tournament selection, arithmetic crossover, and perturbation mutation was applied. The population in each generation consisted of 36 individuals, and the algorithm was terminated after 100 generations. The algorithm determined solution points which, at the end of each generation, were evaluated for their membership in the compromise set according to relation (4). This evaluation was also repeated after all generations to determine the final compromise set. The solutions obtained in individual generations form the initial compromise set, while the solutions obtained after all generations constitute the final compromise set.

The obtained results, in the form of three projections of the three-dimensional compromise set (initial and final) onto the planes of individual criteria, are presented in Figures 8–10. The projections also include a point labeled X, representing the single-objective optimization result described in Section 5.2.

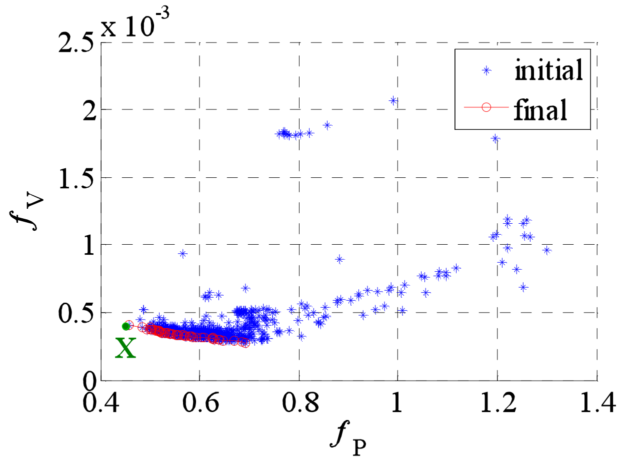

Figure 8: Projection of the compromise set onto the plane f_P–f_V

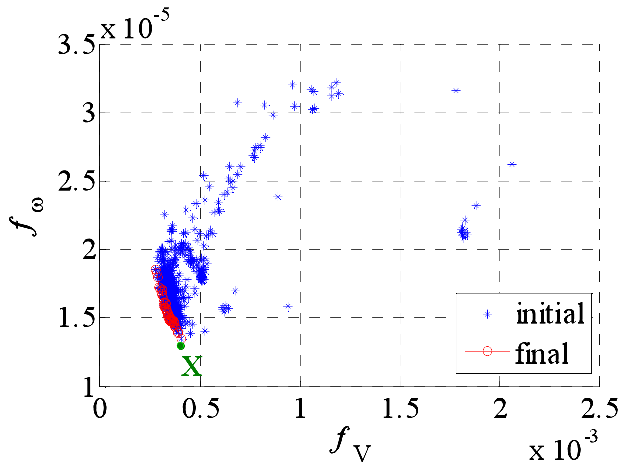

Figure 9: Projection of the compromise set onto the plane f_V–f_ω

As can be observed, the projection of the compromise set (both the initial and final) onto the f_P–f_ω plane indicates that the two criteria – deviations of active

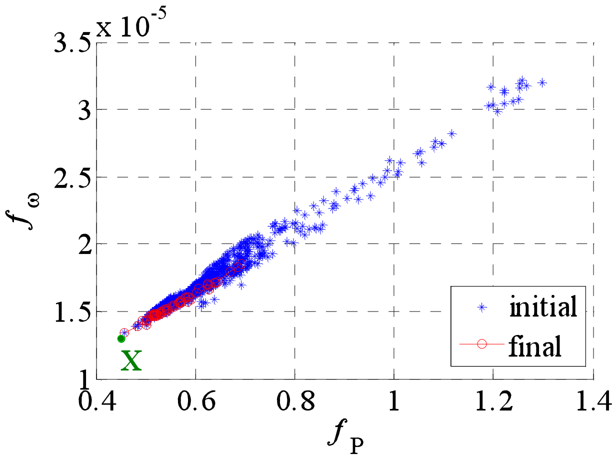

Figure 10: Projection of the compromise set onto the plane f_P–f_ω

power (f_P) and angular speed (f_ω) – are strongly correlated and therefore non-conflicting in practice. This results from the fact that instantaneous power and generator angular speed waveforms are both associated with electromechanical swings in the PS. The relationship between them is approximately linear, which means that the value of one criterion can be determined with high accuracy based on the value of the other. This dependence can be expressed as:

$$f_P \approx a f_\omega \,, \tag{9}$$

where a is a proportionality constant.

Consequently, to simplify the computations, poly-optimization can be carried out using only two criteria, with the following expression adopted as the objective function:

$$\boldsymbol{f} = \begin{cases} f_1 \\ f_2 \end{cases} = \begin{cases} f_P \\ f_V \end{cases} = \begin{cases} \sum\limits_{j=1}^{N_i} \sum\limits_{i=1}^{n} \left| w_{pj} \Delta P_{ij} \right|^2 \\ \sum\limits_{j=1}^{N_i} \sum\limits_{i=1}^{n} \left| \Delta V_{ij} \right|^2 \end{cases} \tag{10}$$

The same genetic algorithm as for objective function (8) was used for the poly-optimization of objective function (10). The obtained results, in the form of the compromise set, are presented in Figure 11.

Figure 12 shows the optimal parameter values (initial and final) of one selected power system stabilizer. The stabilizer installed in generator G3 is used as an example.

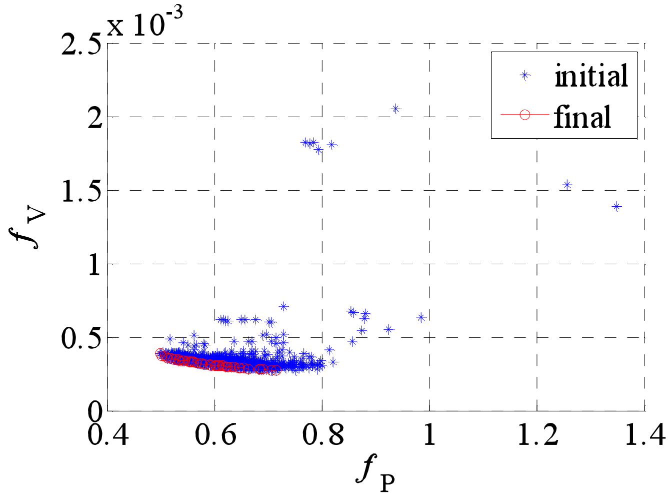

Figure 11: Two-dimensional compromise set

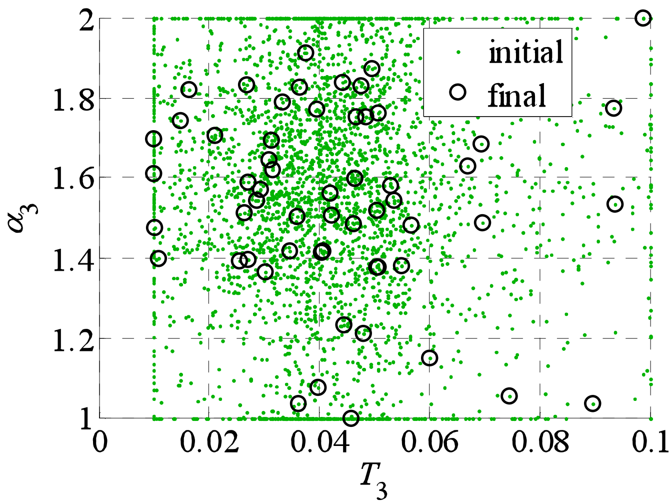

Figure 12: Optimal parameter values of one selected power system stabilizer installed in generator G3

The poly-optimization process results in a set of parameter combinations for the optimized power system stabilizers. The final step is to select a single parameter set that best reflects the requirements imposed on the stabilizers. Since the presented study concerns a general case, three representative solutions were selected as the outcome of poly-optimization. These include two extreme solutions and one intermediate solution from the two-dimensional compromise set.

These points (A, B, and C) are indicated in Figure 13. The point representing the single-objective optimization result described in Section 5.2 is also marked (as X).

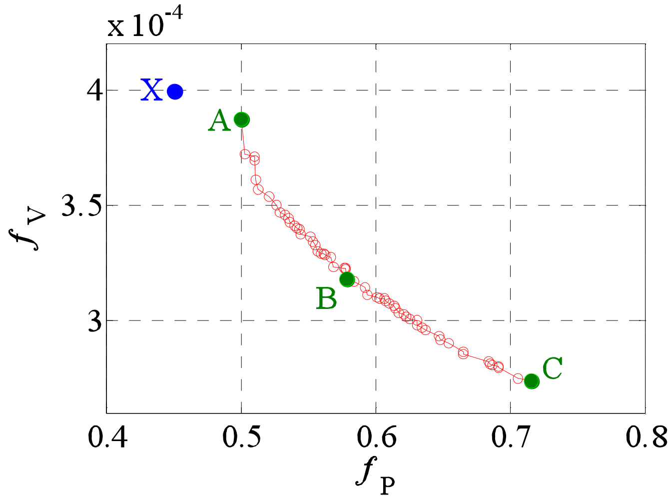

Figure 13: Two-dimensional compromise set

The parameter values of all optimized power system stabilizers for the selected points are presented in Table 4 (the values for the point X are given in Table 3).

Table 4: Calculation results of PSS3B_FRAC power system stabilizer parameters in the 7-machine system – poly-optimization results

point		G1	G2	G3	G4	G5	G6	G7
A	T_3	0.015099	0.011783	0.029309	0.037582	0.026857	0.067868	0.068059
	α_3	1.0943	1.7368	1.572	1.7351	1.5234	1.6284	1.299
B	T_3	0.068007	0.025025	0.027055	0.067949	0.051066	0.030863	0.032452
	α_3	1.4086	1.7203	1.3966	1.9988	1.7326	1.4585	1.5758
C	T_3	0.089066	0.035182	0.031606	0.048091	0.065589	0.037383	0.062962
	α_3	1.5579	1.7958	1.6191	1.5154	1.4431	1.9992	1.9988

As an example, Figures 14 and 15 show the waveforms in case of the D1 disturbance in transmission line L11 of instantaneous power, generator voltage, and angular speed of the generating units G1 and G7 for stabilizers with parameters corresponding to the points A, B, and C (representative poly-optimization results), as well as the point X (the single-objective optimization result for stabilizers in the multi-machine system).

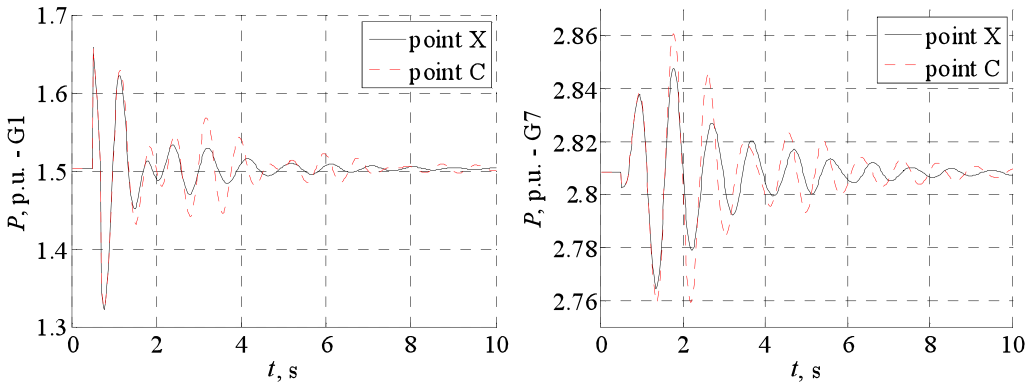

(a)

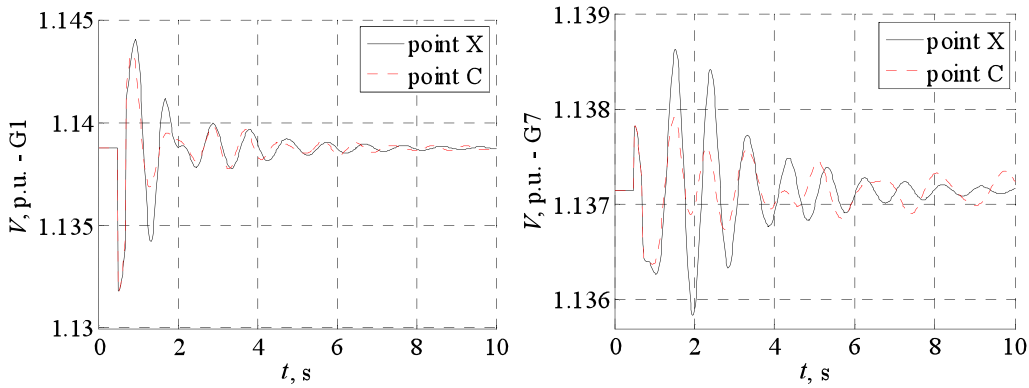

(b)

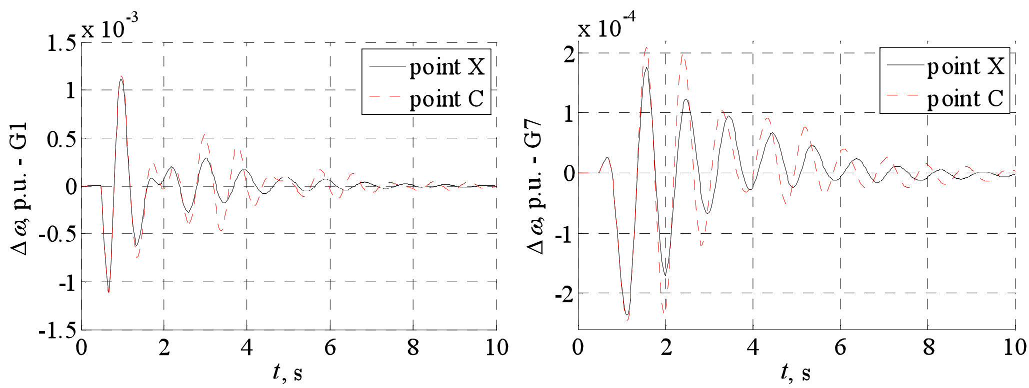

(c)

Figure 14: Waveforms of instantaneous power (a), generator voltage (b), and angular speed (c) of generating units G1 and G7 in the CIGRE system for the points X and C

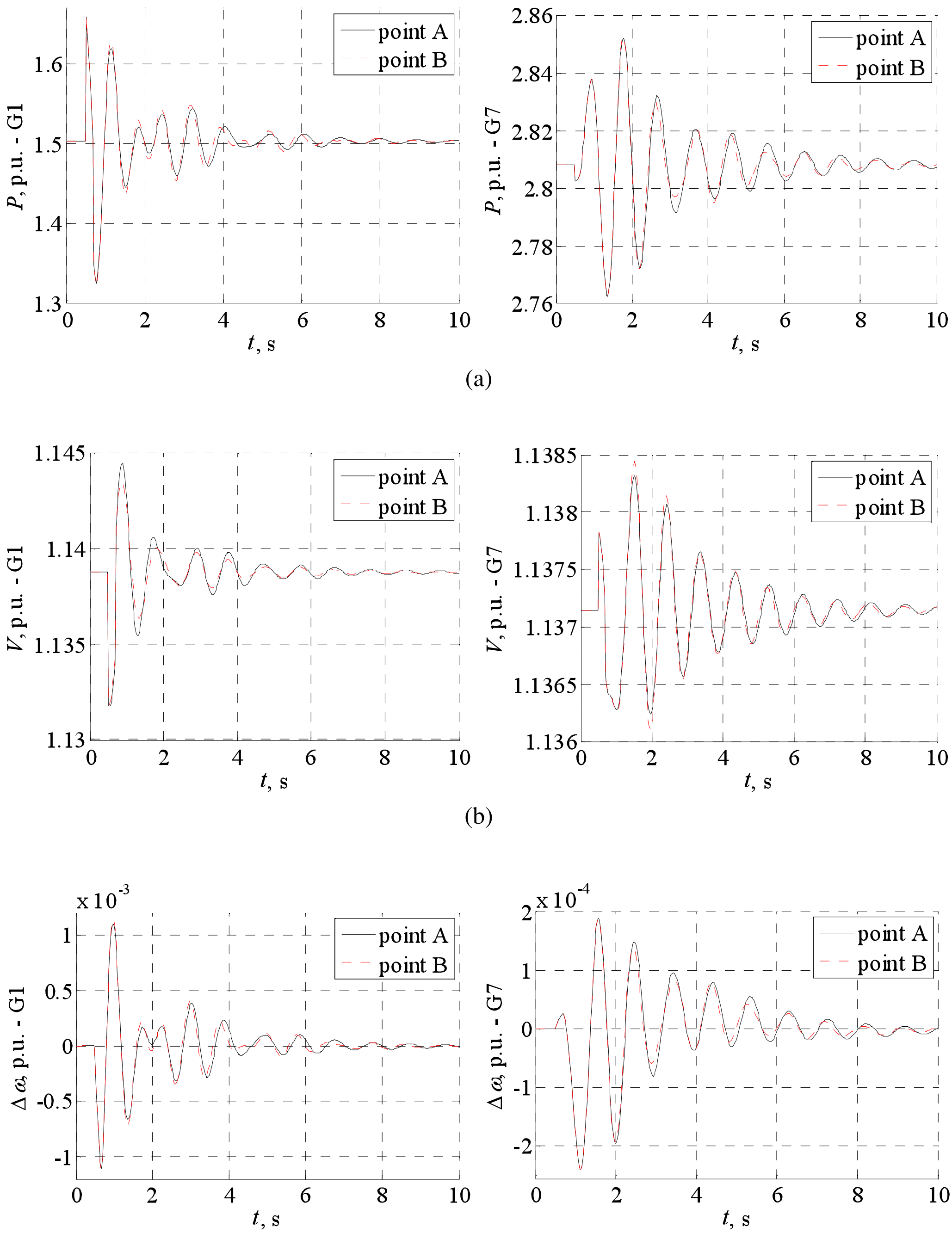

(a) (b) (c)

Figure 15: Waveforms of instantaneous power (a), generator voltage (b), and angular speed (c) of generating units G1 and G7 in the CIGRE system for the points A and B

6. Discussion of results

This paper defines the structure of a new fractional-order power system stabilizer, the PSS3B_FRAC, based on a modification of the structure of a typical PSS3B stabilizer. Examples of the use of this type of stabilizer for damping electromechanical swings in single-machine and multi-machine power systems are presented. The performance of the fractional-order stabilizers, the PSS3B_FRAC, and the traditional PSS3B are compared.

The calculations were divided into three stages:

- In the first stage, all generating units included in the 7-machine CIGRE PS were analyzed separately. The time constants (of the PSS3B_FRAC and PSS3B stabilizers) and the order of actual differentiation of the PSS3B_FRAC stabilizers in the instantaneous power input path were calculated by analyzing single-machine systems (generating unit – bus system) and minimizing the objective function (1).
- In the second stage, improved values selected parameters were calculated: the time constant T_3 and the order of actual differentiation of the PSS3B_FRAC stabilizers in the instantaneous power input path α_3, analyzing the 7-machine CIGRE system and minimizing the objective function (2).
- In the third stage, poly-optimization was carried out for two different objective functions. In the first case, three criteria were optimized, and in the second case two criteria. Based on this, compromise sets were determined, and for selected points, the results were presented in the form of instantaneous power, voltage, and angular speed waveforms of the generators in the multi-machine system.

The obtained results confirm that the proposed multi-stage procedure enables systematic parameter selection and creates a basis for further comparative evaluation of fractional- and integer-order stabilizers in both single- and multi-machine systems.

7. Conclusions

Based on the research, the following conclusions were drawn:

- Fractional-order stabilizers PSS3B_FRAC with appropriately selected parameters effectively damp electromechanical swings in single-machine and multi-machine PS.
- By analyzing single-machine systems, a generating unit – bus system, it is possible to determine a set of parameters of the PSS3B_FRAC and PSS3B power system stabilizers for which the waveforms of instantaneous power, angular speed and node voltages in single-machine and multi-machine PS are satisfactory.

- By performing additional analysis and minimizing the objective function (2), it is possible to further increase the damping of electromechanical swings and improve the waveforms of node voltages in multi-machine PS (objective function values in Table 3).
- Analyzing the calculation results obtained (objective function values in Tables 1 and 2 and waveforms in Figure 7) it can be concluded that with the correct selection of parameters, PSS3B_FRAC stabilizers better damp electromechanical swings and improve node voltage waveforms than traditional PSS3B stabilizers.
- Using multi-criteria optimization allows for further improvement of instantaneous power, angular speed, and voltage waveforms in generating units. The use of multi-criteria optimization allows for the consideration of multiple, sometimes contradictory, requirements without compromising the ability to achieve an optimal solution.
- The criteria f_{P} and f_{ω}, associated with electromechanical swings, that is, the instantaneous power and angular speed waveforms of the generators, exhibit similar characteristics and are approximately proportional to each other (Figure 10 and relation (9)). In a system where instantaneous power is well damped, the angular speed is likewise effectively damped.
- The criterion f_{V}, associated with generator voltage deviations, is usually conflicting with the criteria related to electromechanical swings, f_{P} and f_{ω} (Figures 8 and 9). When electromechanical swings are well damped (for example, at point X of the compromise set in Figure 13), significant voltage deviations typically occur in the network nodes, and vice versa (for example, at point C of the compromise set in Figure 13).
- For a properly conducted poly-optimization, it is possible to select a solution in which all criteria are satisfied to an acceptable degree (in the considered case, the compromise set contains a solution that provides sufficiently good damping of power swings without deteriorating voltage waveforms, e.g., the solution corresponding to point B in the compromise set shown in Figure 13). One may also choose a solution that better satisfies those criteria which are considered more important in a given application.
- It is difficult to observe significant differences between the waveforms (Figures 14 and 15), even though the objective function values vary considerably for the analyzed points of the compromise set (compare the locations of the points A, B, C, and X in Figure 13). This can be explained by the form of objective functions (8) and (10). These functions are based on summing the deviations of the considered quantities for all generating units operating in the analyzed PS. Consequently, the resulting value of the objective function represents a certain averaging of the individual waveforms, and achieving a

clearly noticeable improvement in the waveforms would require optimization of the objective function (6) or a substantial increase in the number of generations in the genetic algorithm [31].

- The single-objective optimization result associated with the minimization of objective function (2) corresponds to a single point in the three-dimensional compromise set, as shown in Figures 8–10. The weighting coefficients of objective function (2) were selected such that the stabilizers with parameters resulting from its minimization provide good damping of generator voltage waveforms, while electromechanical waveforms (e.g., instantaneous power) are damped less effectively (Figure 14).
- A configuration with multiple criteria provided better suppression of power swings, as indicated by reduced f_P values, relative to the two-criterion poly-optimization case. However, it cannot be clearly stated whether this improvement was caused solely by the increased number of criteria. A probable reason may also be the imperfection of the genetic algorithm, which does not always explore all regions of the objective space. Another contributing factor is the fact that the relationship between f_P and f_ω is only approximately linear (relation (9)). This also helps explain the location of point X in Figure 13, which should theoretically belong to the compromise set, but the genetic algorithm using two criteria in objective function (10) did not explore that region of the objective space.
- The genetic algorithm used in the analysis explores solutions across the entire control space, including its boundaries (constraints), as can be observed in Figure 12 (points corresponding to the initial compromise set – green points). However, it is difficult to identify a clear relationship between the positions of individual optimal points. This may result from certain limitations of the algorithm, the significant influence of its stochastic operations (especially mutation), and the discrete nature of the compromise set [30].

The presented approach demonstrates that extending the classical PSS3B structure with fractional-order differentiation and multi-stage optimization provides a flexible framework for improving power system dynamic performance.

References

[1] R. Agarwal, S. Hristova and D. O'Regan: Basic concepts of Riemann–Liouville fractional differential equations with non-instantaneous impulses. *Symmetry*, **11**(5), (2019), 614. DOI: 10.3390/sym11050614

[2] R. AlAhmad: Grünwald-Letnikov fractional derivative for a product of two functions. *International Journal of Mathematics and Computer Science*, **16**(2), (2021), 767–774.

[3] T. Białoń, R. Niestrój and W. Korski: PSO-based identification of the Li-Ion battery cell parameters. *Energies*, **16**(10), (2023), 1–22. DOI: 10.3390/en16103995

[4] B. Boudjehem, D. Boudjehem and H. Tebbikh: Simple analytical design method for fractional-order controller. *3-rd IFAC Workshop on Fractional Differentiation and its Applications*, Ankara, Turkey, (2008).

[5] H. Delavari and K. Flahzadeh: Robust fractional order adaptive power system stabilizer for a multi-machine system. *27th Iranian Conference on Electrical Engineering (ICEE)*, Yazd, Iran, (2019), 544–548. DOI: 10.1109/IranianCEE.2019.8786552

[6] T. Dinh, S. Kamal and R. Pandey: Fractional-order system: control theory and applications. *Fractal Fract.*, **7**(1), (2023), 48. DOI: 10.3390/fractalfract7010048

[7] G. Fan, F. Yang, P. Guo, C. Xue, S.G. Farkoush and M.J. Karimpoor: A new model of connected renewable resource with power system and damping of low frequency oscillations by a new coordinated stabilizer based on modified multi-objective optimization algorithm. *Sustain. Energy Technol. Assess.*, **47**, (2021), 101356. DOI: 10.1016/j.seta.2021.101356

[8] M.J. Gibbard: Coordinated design of multimachine power system stabilisers based on damping torque concepts. *IEE Proceedings*, **135**, Pt. C(4), (1988), 276–284.

[9] M. Gocki, A. Jakubowska-Ciszek and P. Pruski: Comparative analysis of a new class of symmetric and asymmetric supercapacitors constructed on the basis of ITO collectors. *Energies*, **16**(1), (2023), 306. DOI: 10.3390/en16010306

[10] IEEE STd 421.5: *IEEE Recommended Practice for Excitation System Models for Power System Stability Studies*, (2016).

[11] T. Kaczorek: Zeroing of state variables in fractional descriptor electrical circuits by state-feedbacks. *Archives of Electrical Engineering*, **63**(3), (2014), 321–333. DOI: 10.2478/aee-2014-0024

[12] M. Khaleghi, M.M. Farsangi, H. Nezamabadi-pour and K.Y. Lee: Pareto-optimal design of damping controllers using modified artificial immune algorithm. *IEEE Transactions on Systems, Man, and Cybernetics, Part C (Applications and Reviews)*, **41**(2), (2011), 240–250. DOI: 10.1109/TSMCC.2010.2052241

[13] Z.E. Khalil, A.E.F. El-Said Eliwa and W. Sabry: A design of a modified power system stabilizer for power system transient stability enhancement. *Twentieth International Middle East Power Systems Conference (MEPCON)*, Cairo, Egypt, (2018), 712–717. DOI: 10.1109/MEPCON.2018.8635297

[14] D. Khanh, P. Vasant, I. Elamvazuthi and V. Dieu: Optimization of thermo-electric coolers using hybrid genetic algorithm and simulated annealing. *Archives of Control Sciences*, **24**(2), (2014), 155–176. DOI: 10.2478/acsc-2014-0010

[15] P. Kundur: *Power system stability and control*, McGraw-Hill, Inc., 1994.

[16] J. Machowski, Z. Lubośny, J. Bialek and J. Bumby: *Power system dynamics. Stability and control*. John Wiley & Sons, New York, 2020.

[17] Ł. Majka: Applying a fractional coil model for power system ferroresonance analysis. *Bulletin of the Polish Academy of Sciences Technical Sciences*, **66**(4), (2018), 467–474. DOI: 10.24425/124263

[18] Mathworks, Inc.: *Optimization Toolbox Documentation*.

[19] Mathworks, Inc.: *Simulink user guide*.

[20] F.P. De Mello and Ch. Concordia: Concepts of synchronous machine stability as affected by excitation control. *IEEE Trans. on Power Systems*, **PAS-88**(4), (1980), 316–329.

[21] Z. Michalewicz, T.D. Logan, and S. Swaminathan: Evolutionary operators for continuous convex parameter spaces. *3rd Annual Conference on Evolutionary Programming*, A.V. Sebald and L.J. Fogel (editors), World Scientific Publishing, River Edge, N.J., (1994), 84–97.

[22] B.L. Miller and D.E. Goldberg: Genetic algorithms, tournament selection, and the effects of noise. *Complex Systems*, **9**(3), (1995), 193–212.

[23] W. Mitkowski and P. Skruch: Fractional-order models of the supercapacitors in the form of RC ladder networks. *Bulletin of the Polish Academy of Sciences Technical Sciences*, **61**(3), (2013), 581–587. DOI: 10.2478/bpasts-2013-0059

[24] B. Mohandes, Y.L. Abdelmagid and I. Boiko: Development of PSS tuning rules using multi-objective optimization. *International Journal of Electrical Power & Energy Systems*, **100**, (2018), 449–462. DOI: 10.1016/j.ijepes.2018.01.041

[25] A. Nocoń and S. Paszek: A Comprehensive Review of Power System Stabilizers. *Energies*, **16**, (2023), 1945, DOI: 10.3390/en16041945

[26] A. Nocoń and S. Paszek: Synthesis of generator voltage regulator when applying poly-optimisation. *Bulletin of the Polish Academy of Sciences Technical Sciences*, **55**, (2007), 43–48.

[27] A. Nocoń, S. Paszek and P. Pruski: Multi-criteria optimization of the parameters of PSS3B system stabilizers operating in an extended power system with the use of a genetic algorithm. *Archives of Control Science*, **32**(2), (2022), 233–255. DOI: 10.24425/asc.2022.141711

[28] M. Panda, B. Das and B. Pati: Global path planning for multiple AUVs using GWO. *Archives of Control Sciences*, **30**(1), (2020), 77–100. DOI: 10.24425/acs.2020.132586

[29] M. Peschel and C. Riedel: *Poly-optimierung – eine Entscheidungshilfe für ingenieurtechnische Kompromislösungen*. VEB Verlag Technik, Berlin, 1976 (in German).

[30] S. Paszek and A. Nocoń: *Optimisation and Poly-optimisation of Power System Stabilizer Parameters*. Lambert, Saarbrucken, 2014.

[31] S. Paszek and A. Nocoń: Parameter poly-optimization of PSS2A power system stabilizers operating in a multi-machine power system including the uncertainty of model parameters. *Elsevier, Applied Mathematics and Computation*, **267**, (2015), 750–757. DOI: 10.1016/j.amc.2014.12.013

[32] Power Technologies, a Division of S&W Consultants Inc., *Program PSS/E Application Guide*. Siemens Power Technologies Inc., 2002.

[33] P. Pruski and S. Paszek: Location of generating units most affecting the angular stability of the power system based on the analysis of instantaneous power waveforms. *Archives of Control Science*, **30**(2), (2020), 273–293. DOI: 10.24425/acs.2020.133500

[34] S. Racewicz, F. Kutt, M. Michna and Ł. Sienkiewicz: Comparative study of integer and non-integer order models of synchronous generator. *Energies*, **13** (2020), 4416. DOI: 10.3390/en13174416

[35] S. Robak, K. Gryszpanowicz, M. Piekarz and M. Polewaczyk: Transient stability enhancement by series braking resistor control using local measurements. *Elsevier, Electrical Power and Energy Systems*, **112**, (2019) 272–281. DOI: 10.1016/j.ijepes.2019.05.015

[36] S. Robak, J. Machowski and M. Skwarski: Enhancement of power system stability by real-time prediction of instability and early activation of steam turbine fast valving. *Energy Reports*, **8**, (2022), 7704–7711. DOI: 10.1016/j.egyr.2022.05.285

[37] S. Robak, J. Machowski, A. Smolarczyk and M. Skwarski: Transient stability improvement by generator tripping and real-time instability prediction based on local measurements. *IEEE Access*, **9**, (2021), 130519–130528. DOI: 10.1109/ACCESS.2021.3111967

[38] M. Saadatmand, B. Mozafari, G.B. Gharehpetian and S. Soleymani: Optimal coordinated tuning of power system stabilizers and wide-area measurement-based fractional-order PID controller of large-scale PV farms for LFO damping in smart grids. *International Transactions on Electrical Energy Systems*, **31**, (2021), e12612. DOI: 10.1002/2050-7038.12612

[39] I. Schäfer and K. Krüger: Modelling of lossy coils using fractional derivatives. *Journal of Physics D: Applied Physics*, **41**(8), (2008), 8. DOI: 10.1088/0022-3727/41/4/045001

[40] D. Sierociuk, M. Malesza and M. Macias: *Fractional Variable Order Derivative Simulink Toolkit ver. 3.00 User Guide*, Warsaw University of Technology, 2019, https://www.mathworks.com/matlabcentral/fileexchange/38801-fractional-variable-order-derivative-simulink-toolkit

[41] D. Spałek: Synchronous generator model with fractional order voltage regulator PIbDa. *Acta Energetica*, **23**(2), (2015), 78–84. DOI: 10.12736/issn.2300-3022.2015208

[42] A.V. Tare, L.D. Mahajan, V.N. Pande and V.A. Vyawahare: Fractional-order modeling and control of power system stabilizer. *IEEE International Conference on Industrial Technology (ICIT)*, Melbourne, Australia, (2019), 625–630. DOI: 10.1109/ICIT.2019.8755134

[43] A. Tare, P. Patil and V. Pande: Design of fractional-order power system stabilizer. *8th International Conference on Power Systems (ICPS)*, Jaipur, India, (2019), 1–6. DOI: 10.1109/ICPS48983.2019.9067638

[44] V. Vesely, J. Osusky and I. Sekaj: Gain scheduled controller design for thermo-optical plant. *Archives of Control Sciences*, **24**(3), (2014), 333–349. DOI: 10.2478/acsc-2014-0020

[45] Y. Zhang, J. Yu, N. Zhao, Z. Xu, Y. Yan, D. Wu, K. Blacktop and A. Tsolakis: Particle swarm optimization for a hybrid freight train powered by hydrogen or ammonia solid oxide fuel cells. *International Journal of Hydrogen Energy*, **72**, (2024), 626–641. DOI: 10.1016/j.ijhydene.2024.05.347